# Lip-field approach for modeling strain softening in viscoelastic materials

Rajasekar Gopalsamy, Nicolas Chevaugeon, Olivier Chupin, Jean Michel Piau, Ferhat Hammoum

# Lip-field approach for modeling fracture in viscoelastic materials

**Rajasekar Gopalsamy[a], Nicolas Chevaugeon[b], Olivier Chupin[a], Jean-michel Piau[a], Ferhat Hammoum[c]**

a. Univ Gustave Eiffel, MAST-LAMES, F-44344 Bouguenais, France
rajasekar.gopalsamy@univ-eiffel.fr, olivier.chupin@univ-eiffel.fr, jean-michel.piau@univ-eiffel.fr
b. Ecole Centrale de Nantes, GeM Institute, UMR CNRS 6183,1 rue de la Noe, 44321 Nantes, France
nicolas.chevaugeon@ec-nantes.fr
c. Univ Gustave Eiffel, MAST-MIT, F-44344 Bouguenais, France
ferhat.hammoum@univ-eiffel.fr

## Résumé :

*La rupture des matériaux visoélastiques est considérée comme un phénomène complexe en raison de leur comportement hautement sensible à la vitesse et à la température. Le présent article vise à modéliser la rupture dans les solides viscoélastiques pour différents taux de chargement et conditions de température. Dans un premier temps, un modèle viscoélastique linéaire basé sur le formalisme des matériaux standards généralisés est considéré. Dans un second temps, une variable d'endommagement est introduite dans le modèle dans le cadre de la Mécanique d'Endommagement Continu (CDM) et régularisée par l'approche Lip-field. Enfin, des simulations numériques sont effectuées pour différents taux de chargement et températures, les effets de la température étant pris en charge par le principe de superposition temps-température (TTSP). Les résultats démontrent la capacité du modèle à représenter qualitativement le comportement typique des matériaux viscoélastiques.*

## Abstract :

*Fracture of visoelastic materials is considered to be a complex phenomenon due to their highly rate and temperature sensitive behaviour. The present paper aims to model fracture in viscoelastic solids for different loading rate and temperature conditions. First, a linear viscoelastic model based on the formalism of generalized standard materials is considered. Second a damage variable is introduced into the model within the framework of Continuum Damage Mechanics (CDM) and regularized through the Lip-field approach. Finally, numerical simulations are performed for different loading rate and temperature with the temperature effects taken care of by the Time Temperature Superposition Principle (TTSP). Results demonstrate the ability of the model to qualitatively represent the typical behavior of the viscoelastic materials.*

**Key words : fracture, localization, damage, viscoelasticity, Lip-field**

# 1 Introduction

Viscoelastic materials like asphalt, biological tissues,wood and polymers have numerous applications in engineering. Almost all materials exhibit viscoelastic behavior when the considered time scale is large enough. The properties of these materials are highly rate and temperature dependent that hence largely affect their failure behavior [1, 2]. Design for mitigation of fracture in viscoleastic materials is an important problem for e.g. in case of asphalt and pavement construction [3].

A detailed review of viscoelastic fracture was presented by Knauss [4]. Several works have been done in the past for the modeling of fracture in viscoelastic solids. Schapery [5, 6] used the correspondence principle [7] to define a generalized time dependent J-integral for fracture in viscoelastic material analogous to the elastic case. Based on this theory, a new model was proposed in [8] to study the creep fracture in viscoelastic materials.

Several numerical methods have been developed to study the failure behavior of different materials caused by crack propagation. They can be broadly classified into discrete fracture mechanics based approach and damage mechanics based approach. In discrete approach, X-FEM [9, 10] has gained a lot of attention in the past. X-FEM approach was used in [11, 12] to address linear viscoelasticity problems with inclusions and cracks. Damage mechanics based approach can further be broadly categorised as Cohesive Zone Model (CZM) [13, 14] and Continuum Damage Mechanics (CDM) [15, 16]. Both approaches account for the micro-damage before fracture that can be associated to the nucleation, coalescence and growth of voids to form macro-cracks. Some works on use of CZM to model viscoelastic fracture can be found in [17, 18]. CDM is another popular approach for modeling damage in viscoelastic materials. Some of the commonly used CDM approaches are non-local integral damage models [20, 19], phase field damage models [21, 22] and Thick Level Set(TLS) approach [23]. For e.g. Shiferaw et al [24] used the TLS approach for modeling damage in viscoelastic materials for a wide range of temperature. Phase field models have also been used to model cracks in viscoelasticity [27, 25, 26]. Another class of method that was recently developed under the formalism of CDM was the Lip-field approach [28, 29] to fracture. The main difference of this approach from the phase field approach lies in the fact that damage energy functional is not a function of the damage gradient.

Fracture behavior of viscoelastic materials (e.g. bituminous materials) is a complex phenomenon due to their highly rate-sensitive and temperature-dependent behavior. Modeling of such fracture behavior in viscoelasticity for a wide range of loading and temperature conditions can still be considered to be a relatively open area. This lays the objective of the present paper. Initially a viscoelastic model based on the formalism of generalized standard materials [30, 31] is proposed by defining the respective free energy and viscous dissipation potentials. In particular, the Generalized Kelvin-Voigt (GKV) model [7] is used to represent the viscoelastic behaviour. The temperature effects are taken care of by the Time Temperature Superposition Principle (TTSP) [32, 7]. Then an isotropic damage variable is being introduced into the model based on the formalism of CDM. Further, an incremental potential is proposed by gathering the respective free energy and dissipative potentials. This leads to the variational formulation of the problem under consideration, with the minimization of the incremental potential providing the solution of the mechanical problem. Finally, the mechanical problem is regularized by the introduction of a length scale using the Lip-field approach. We keep the discussion of the numerical aspects of the Lip-field approach to minimal and the details can be found in [28, 29].

The paper is organized as follows : The Lip-field regularized viscoelastic damage model is described in the next section. In Section 3, the numerical aspects are briefed. Numerical results are then presented

in Section 4 for different loading rates and temperature. Finally, the paper concludes with summary and possible future works.

## 2 The mechanical model

Consider the deformation of a body initially occupying a domain $\Omega$ through a displacement field $\mathbf{u}$. We assume small, quasi-static deformations under isothermal conditions. The Cauchy stress and small strain tensor is denoted as $\boldsymbol{\sigma}$ and $\boldsymbol{\varepsilon}$.

$$\boldsymbol{\varepsilon(u)} = \frac{1}{2}(\nabla \mathbf{u} + \nabla^T \mathbf{u}) \tag{1}$$

Regarding the boundary conditions, the displacement is applied on a part of the boundary $\Gamma_u$. On the rest of boundary $\Gamma_N$, zero traction forces are assumed. We also assume that there is no body force. To be kinematically admissible at any given time $t$, the displacement field must belong to $U(t)$ :

$$U(t) = \{\mathbf{u} \in H^1(\Omega) : \mathbf{u} = \mathbf{u_d}(t) \ \ on \ \ \Gamma_u\} \tag{2}$$

The equilibrium condition then reads

$$\int_\Omega \boldsymbol{\sigma} : \boldsymbol{\varepsilon}(\mathbf{u}^*)\, d\Omega = 0, \quad \forall\, \mathbf{u}^* \in U^* \quad U^* = \{\mathbf{u} \in H^1(\Omega) : \mathbf{u} = 0 \ \ on \ \ \Gamma_u\} \tag{3}$$

The equilibrium and the kinematic equations Eq. (2) and (3) must be complemented with the constitutive equations. For the constitutive behaviour, we consider the Generalized Kelvin Voigt (GKV) model [7]. The schematic of GKV model in 1D case is shown in Fig. 1, where $\boldsymbol{\varepsilon_1}, \boldsymbol{\varepsilon_2}, ..., \boldsymbol{\varepsilon_n}$ are the internal variables associated with the viscous strain in each Kelvin Voigt (KV) unit. $E_0, E_1, .., E_n$ and $\tau_1, ..., \tau_n$ represent the spring constants and retardation times of the dashpots respectively. We assume that the Poisson's ratio $\nu$ is constant for all Kelvin-Voigt units (and time independent).

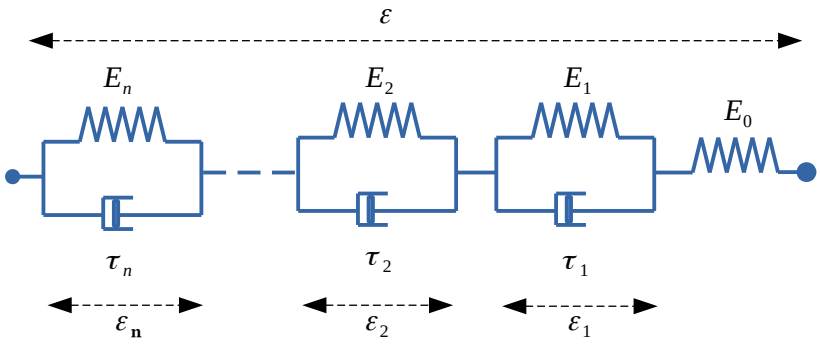


FIGURE 1 – Generalized Kelvin Voigt (GKV) model

To account for the effects of temperature, time-temperature superposition principle [7] is used. This allows to use the Williams–Landel–Ferry (WLF) [32] equation to find the shift factor $\alpha_T$ as follows :

$$log(\alpha_T) = \frac{-C1(T - T_{ref})}{C2 + T - T_{ref}} \tag{4}$$

where $C1$ and $C2$ are the material constants. The shift factor proportionally alters the retardation time to account for the changes in temperature as follows : $\tau_i(T) = \alpha_T(T)\tau_i(T_{ref})$.

We will use the formalism of Generalized Standard Materials [30, 31] to describe the constitutive behaviour. The model is characterised by the free energy potential $\psi(\boldsymbol{\varepsilon}(\mathbf{u}), \boldsymbol{\varepsilon_1}, ..., \boldsymbol{\varepsilon_n})$ and the (viscous) dissipation potential $\phi(\dot{\boldsymbol{\varepsilon}}_1, .., \dot{\boldsymbol{\varepsilon}}_n)$. We use the implicit time discretisation. Consider the displacement and internal variables (viscous strains) known at some time $t_m$. Then finding the solution pair $(\mathbf{u_{m+1}}, \boldsymbol{\varepsilon_{1,m+1}}, ..., \boldsymbol{\varepsilon_{n,m+1}})$ at the next time instant $t_{m+1} = t_m + \Delta t$ amounts to the following minimization problem [33].

$$(\mathbf{u}, \boldsymbol{\varepsilon_1}, ..., \boldsymbol{\varepsilon_n}) = \arg \min_{\substack{\mathbf{u}' \in U_m \\ \boldsymbol{\varepsilon_1}', .., \boldsymbol{\varepsilon_n}'}} F(\mathbf{u}', \boldsymbol{\varepsilon_1}', .., \boldsymbol{\varepsilon_n}' \,;\, \mathbf{u_m}, \boldsymbol{\varepsilon_{1,m}}, .., \boldsymbol{\varepsilon_{n,m}}, \Delta t) \tag{5}$$

where $U_m$ is the short hand notation for $U(t_{m+1})$ and we dropped the $m+1$ indices(for the rest of the paper) to simplify the notations. We will also drop the constants and known variables from previous time step in $F$ whenever possible for clarity. The expression for $F$ is follows [33] :

$$F(\mathbf{u}, \boldsymbol{\varepsilon_1}, .., \boldsymbol{\varepsilon_n}) = \int_\Omega \left[ \psi(\boldsymbol{\varepsilon}(\mathbf{u}), \boldsymbol{\varepsilon_1}, ..., \boldsymbol{\varepsilon_n}) + \Delta t \; \phi \left( \frac{\boldsymbol{\varepsilon_1} - \boldsymbol{\varepsilon_{1,m}}}{\Delta t}, .., \frac{\boldsymbol{\varepsilon_n} - \boldsymbol{\varepsilon_{n,m}}}{\Delta t} \right) \right] d\Omega \tag{6}$$

where the time derivative of the viscous strains $\boldsymbol{\varepsilon_i}$ $(i = 1, 2.., n)$ is replaced by the differential quotient $(\boldsymbol{\varepsilon_i} - \boldsymbol{\varepsilon_{i,m}})/\Delta t$. The free energy and dissipation potential are given by

$$\psi = \frac{1}{2} \left( \boldsymbol{\varepsilon} - \sum_{i=1}^{n} \boldsymbol{\varepsilon_i} \right) : \mathbb{E}_0 : \left( \boldsymbol{\varepsilon} - \sum_{i=1}^{n} \boldsymbol{\varepsilon_i} \right) + \sum_{i=1}^{n} \frac{1}{2} \boldsymbol{\varepsilon_i} : \mathbb{E}_i : \boldsymbol{\varepsilon_i} \tag{7}$$

$$\phi = \sum_{i=1}^{n} \frac{1}{2} \dot{\boldsymbol{\varepsilon}}_i : \tau_i \mathbb{E}_i : \dot{\boldsymbol{\varepsilon}}_i \tag{8}$$

where the linear elasticity tensor $\mathbb{E}_i = 2\mu_i \mathbb{I} + \lambda_i \mathbf{1} \otimes \mathbf{1}$ is defined in terms of Lame's constants $\lambda_i$ and $\mu_i$ associated to $i^{th}$ Kelvin-Voigt unit , with $\mathbb{I}$ and $\mathbf{1}$ being the fourth and second order identity tensors respectively. The convexity of the free energy and viscous dissipation potential ensures that the viscous dissipation is positive, thus satisfying the second law of thermodynamics.

An isotropic (internal) damage variable $d$ is introduced into the GKV model within the framework of Continuum Damage Mechanics (CDM) by use of the effective stress principle. $d = 0$ indicates virgin material and $d = 1$ indicates crack. In particular, an energetic degradation function $g(d)$ diminishes the materials capability to store the free energy and dissipate viscous energy to yield the modified incremental potential as follows (with $g(d) : [0, 1] \to [1, 0]$) :

$$F(\mathbf{u}, \boldsymbol{\varepsilon_1}, .., \boldsymbol{\varepsilon_n}, d) = \int_\Omega g(d)\psi(\boldsymbol{\varepsilon}(\mathbf{u}), \boldsymbol{\varepsilon_1}, ..., \boldsymbol{\varepsilon_n}) + \Delta t \; g(d)\phi \left( \frac{\boldsymbol{\varepsilon_1} - \boldsymbol{\varepsilon_{1,m}}}{\Delta t}, .., \frac{\boldsymbol{\varepsilon_n} - \boldsymbol{\varepsilon_{n,m}}}{\Delta t} \right) \; d\Omega \tag{9}$$

In our case, we consider the free energy of the springs as the driving force for the damage. So the evolution of the damage is given by the minimization of a different incremental potential $F_d$ [28, 29]

$$F_d(\mathbf{u}, \boldsymbol{\varepsilon_1}, .., \boldsymbol{\varepsilon_n}, d) = \int_\Omega g(d)\psi(\boldsymbol{\varepsilon}(\mathbf{u}), \boldsymbol{\varepsilon_1}, ..., \boldsymbol{\varepsilon_n}) + Y_c h(d) \; d\Omega \tag{10}$$

where $h(d)$ is a softening function that controls the damage evolution behaviour. As will be seen, both $g(d)$ and $h(d)$ will take user defined convex function so that $F_d$ preserves convexity w.r.t damage variable $d$. Therefore, the solution of the mechanical problem $(\mathbf{u}, \boldsymbol{\varepsilon_1}, .., \boldsymbol{\varepsilon_n}, d)$ at time $t_{m+1}$ can be formulated as the minimization of the two different incremental potentials Eq.(9),(10) as follows :

$$(\mathbf{u}, \boldsymbol{\varepsilon_1}, ..., \boldsymbol{\varepsilon_n}) = \arg \min_{\substack{\mathbf{u}' \in U_m \\ \boldsymbol{\varepsilon_1}', .., \boldsymbol{\varepsilon_n}'}} F(\mathbf{u}', \boldsymbol{\varepsilon_1}', .., \boldsymbol{\varepsilon_n}', d) \tag{11}$$

$$d = \arg \min_{d' \in A_n \cap \mathcal{L}_{\Omega, l_c}} F_d(\mathbf{u}, \boldsymbol{\varepsilon_1}, .., \boldsymbol{\varepsilon_n}, d) \tag{12}$$

The damage irreversibility constraint is given by the space $A_m$.

$$A_m = \{d \in L^\infty(\Omega) : d_m \leq d \leq 1\} \tag{13}$$

The damage irreversibility constraint ensures that the dissipation due to damage is positive. The damage softening models exhibit spurious mesh dependency problems [34]. Hence in our case a length scale $l_c$ is introduced into the model through the Lipschitz regularized space $\mathcal{L}_{\Omega, l_c}$ as explained below : The Lipschitz constant associated to any given damage field $d$ over the domain $\Omega$ is the minimum $M$ such that the following holds

$$|d(\mathbf{x}) - d(\mathbf{y})| \leq M dist(\mathbf{x}, \mathbf{y}) \; \forall \mathbf{x}, \mathbf{y} \in \Omega \tag{14}$$

where $dist(\mathbf{x}, \mathbf{y})$ is the minimal length of the path inside $\Omega$ joining $\mathbf{x}$ and $\mathbf{y}$ (the distance is considered infinite if the two points cannot be connected inside $\Omega$). The value $M$ defined above is denoted $lip(d)$. This leads to the following definition of the Lipschitz regularized space [28]

$$\mathcal{L}_{\Omega, l_c} = \left\{ d \in L^\infty(\Omega) : lip(d) \leq \frac{1}{l_c} \right\} \tag{15}$$

We consider the following energy degradation function and softening function for the rest of the study.

$$g(d) = (1-d)^2 + \alpha(1-d)d^3 \tag{16}$$

$$h(d) = 2d + 3d^2 \tag{17}$$

# 3 Numerical aspects

The mechanical problem under considered is discretized by means of finite elements in space and finite difference in time. The incremental potential $F$ (Eq. (9)) is convex w.r.t $\mathbf{u}, \boldsymbol{\varepsilon_1}, .., \boldsymbol{\varepsilon_n}$ for a fixed damage field $d$ and the incremental potential $F_d$ (Eq. (10)) is convex w.r.t to damage field $d$ for fixed $\mathbf{u}, \boldsymbol{\varepsilon_1}, .., \boldsymbol{\varepsilon_n}$. Hence, a staggered scheme is used in which the minimization (given by Eq. (11) and (12)) is performed alternatively until convergence. It is to be noted that while performing the minimization of $F$ (Eq. (11)), the damage field is kept fixed (and equal to its latest available value) and while performing the minimization of $F_d$ (Eq. (12)), the deformation $\mathbf{u}$ and viscous strains $\boldsymbol{\varepsilon_1}, ..., \boldsymbol{\varepsilon_n}$ are fixed (and equal to the latest available value).To accelerate the minimization process for finding the damage field, we employ a technique detailed in [28, 29]. Briefly, it contains three steps :

1. First a purely local minimization is performed without the Lipschitz constraint to find the trial

damage $\bar{d}$ as follows :

$$\bar{d} = \arg \min_{d' \in A_m} F_d(\mathbf{u}, \boldsymbol{\varepsilon_1}, .., \boldsymbol{\varepsilon_n}, d) \tag{18}$$

2. Then the set of active nodes is found. Active nodes are defined as the nodes where the $\bar{d} \notin \mathcal{L}_{\Omega,l_c}$. $d$ is assigned $\bar{d}$ in all the nodes except for the active nodes.
3. Finally, a global minimization for the damage variable given by Eq. (12) is performed only in the subdomain occupied by active nodes.

Step 2 is done efficiently using a fast marching technique described in [29]. For the Step 3, *cvxopt* [35] library of the Python has been used to impose the damage irreversibility ($A_m$) and Lipschitz constraint ($\mathcal{L}_{\Omega,l_c}$). This library allows to impose the damage constraints in discrete form through first and second order cone constraints.

# 4 Simulation results

A TDCB (Tapered Double Cantilever Beam) geometry shown in Fig. 2 is used for the study. This geometry has already been used in [29] for studying fracture in elasticity using Lip-field approach. This geometry ensures that the crack growth is relatively stable as the imposed displacement increases.

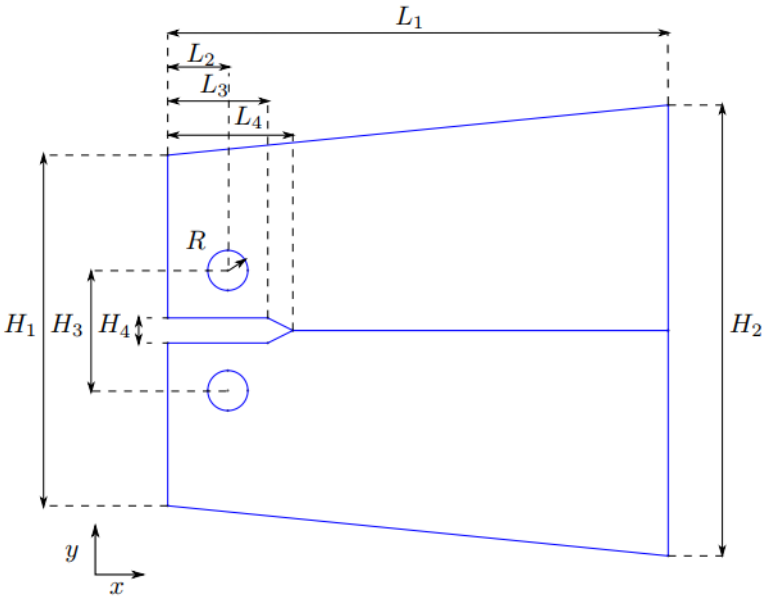


FIGURE 2 – TDCB Geometry specimen

| units | L1 | L2 | L3 | L4 | H1 | H2 | H3 | H4 | R |
|---|---|---|---|---|---|---|---|---|---|
| mm | 100 | 12 | 20 | 24 | 70 | 90 | 24 | 5 | 4 |

TABLE 1 – Dimensions for the TDCB geometry

| KV unit (i) | 0 | 1 | 2 | 3 | 4 | 5 | 6 | 7 | 8 | 9 | 10 | 11 |
|---|---|---|---|---|---|---|---|---|---|---|---|---|
| $E_i(MPa)$ | 31770 | 87398 | 123414 | 65830 | 62457 | 62661 | 7305 | 12500 | 418 | 1743 | 79 | 39 |
| $\tau_{i,ref}$ (s) | N/A | 1E-5 | 1E-4 | 1E-3 | 5E-3 | 1E-2 | 1E-1 | 1 | 10 | 1E2 | 5E2 | 1E3 |

TABLE 2 – Parameters for GKV model

| $Y_c\ (N/m^2)$ | $\nu$ | $\alpha$ | $C_1$ | $C_2\ (^\circ C)$ |
|---|---|---|---|---|
| 30 | .2 | .1 | 29.095 | 211.60 |

TABLE 3 – Material parameters

The dimension for the TDCB geometry is listed in Table 1. The loading in y-direction is applied through linearized rigid body motion on the boundary two holes. We make the assumption of plane strain and isothermal conditions. For the GKV model (viscoelastic model) , the parameters are listed in Table 2 and these values were extracted from [24].The retardation times of the GKV model are listed for the reference temperature $T = 20°C$. The other material parameters of the model are listed in Table 3, where $\nu$ is the Poisson's ratio. It is to be noted that for the present numerical study $Y_c$ is considered constant irrespective of the loading rate and temperature. However this is not the case as observed in experiments. For the assumed plane strain condition, the Lame's constants are found as follows : $\lambda_i = E_i\nu/(1+\nu)/(1-2\nu)$ and $\mu_i = E_i/2/(1+\nu)$. The TDCB geometry is spatially discretized through linear triangular elements (number of nodes = 8112 and number of triangular elements = 15944). We use $l_c = 5\ mm$ to ensure that there are enough elements (10 elements) in the crack band. The time step $dt$ is set to $1e-4\ s$ for all the simulations. The crack length is found approximately as $\int_\Omega d/l_c\ d\Omega$.

## 4.1 Influence of loading rate

Viscoelastic models are rate dependent. We study the influence of the imposed displacement rate on the TDCB specimen to study the rate sensitivity of the considered model. The simulation was performed at $T = T_{ref} = 20°C$ (shift factor $\alpha_T = 1$). We consider the following three imposed loading rates for the study : 1 mm/s, 0.1 mm/s, 0.01 mm/s.

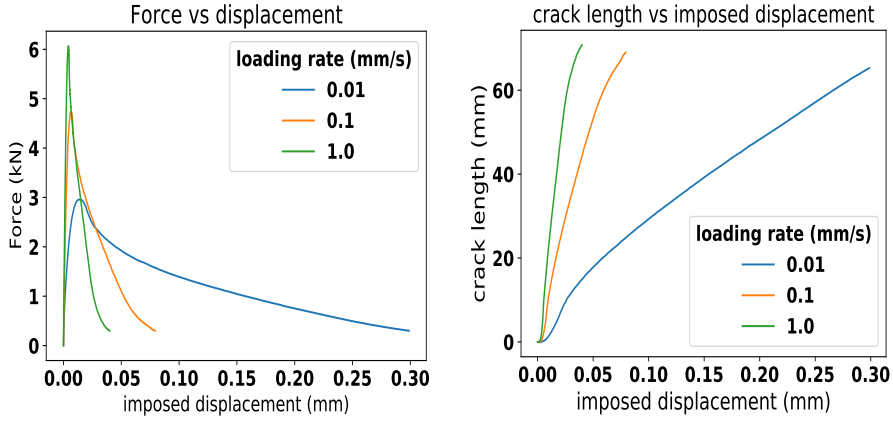


(a) Force vs displacement (b) Crack length vs displacement

FIGURE 3 – Force-displacement plot and crack length - displacement plot for different loading rates

Figure 3 shows the force-displacement curves and crack length vs displacement curve for the considered loading rates. It can be seen from the Figure 3a as the imposed displacement rate increases, the load carrying capacity of the specimen increases and the displacement at rupture decreases, which is a typical response of the viscoelastic materials undergoing fracture. Moreover, Figure 3b shows that the crack grows faster as the imposed displacement rate increases. This can be explained as follows : a) at extreme loading rates (very low and very high loading rates) the viscous dissipation is negligible and most of the dissipation happens through fracture. b) Higher the loading rate higher the stiffness of the model (glassy region) compared to low loading rates (rubbery region). Both in glassy and rubbery regions the model behavior is similar to behavior in elasticity with negligible viscous dissipation, except for the transition region where the viscous dissipation is significant. Hence at extreme loading rates, the model behavior is similiar to elasticity but with different stiffness and hence differenct crack speeds.

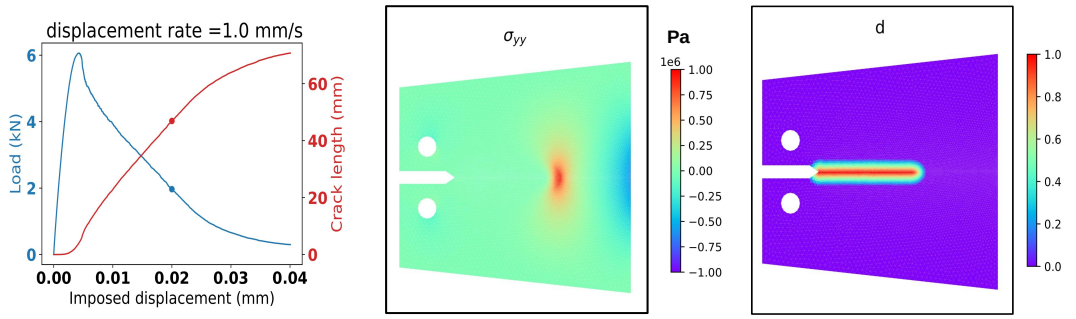


FIGURE 4 – From left to right a) Force-displacement and crack length vs displacement plot b) stress field in y-direction c) damage field (all contour plots showed for $u = .02\ mm$)

Snapshots for the stress in y-direction and damage field (crack band) for the imposed displacement rate of 1 mm/s at $u_{imposed} = .02\ mm$ is shown in Figure 4. It can be seen that the fracture results in mode-I crack pattern with stress being maximum close to the crack tip. It can be seen from Figure 4a that the crack initially grows faster and then it slows down after approximately three quarters of the maximum size of crack.

## 4.2 Influence of temperature

We now study the influence of temperature on the fracture behaviour. We consider the following three different temperatures for the study : $10°C,\ 20°C$ and $30°C$. The difference in temperature is accounted for in the model by shifting the retardation times $\tau_i$ by the shift factor $\alpha_T$ calculated using the WLF equation (Eq. (4)).

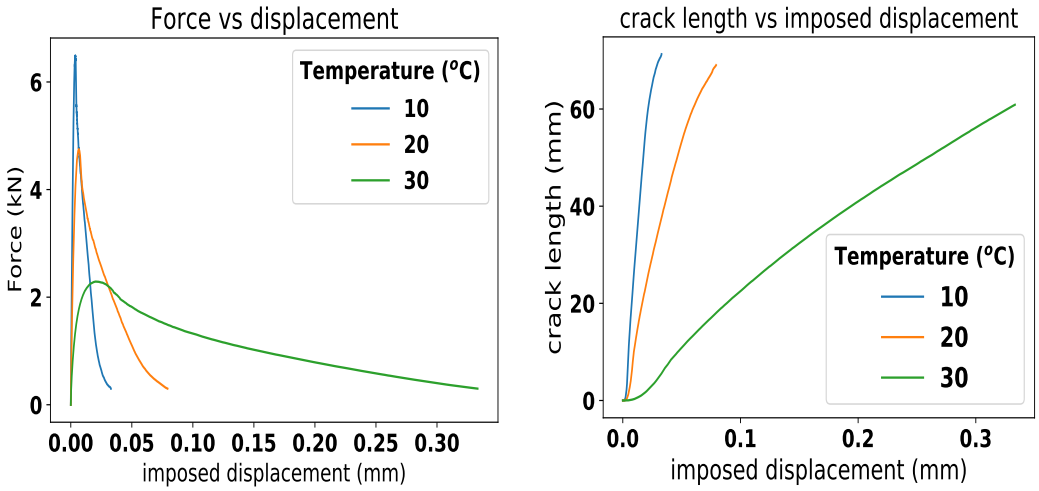


(a) Force vs displacement

(b) Crack length vs displacement

FIGURE 5 – Force- and crack length- displacement plots for different temperature at $\dot{u}_{imposed} = .1$ mm/s.

Figure 5 shows the force displacement curves and crack-length vs imposed displacement for different temperatures for fixed imposed displacement rate of .1 mm/s. It can be seen that as the temperature increases the load carrying capacity of the model decreases and the rate of increase of crack length decreases. Moreover, it can be observed that increase in temperature has similar (qualitative) effect as decrease in loading rate, which is typical to viscoelastic materials.

# 5 Conclusion

The paper described a viscoelastic damage model being implemented within the variational framework and regularized using the Lip-field approach. The numerical results produced for various loading rates and temperature conditions exhibit the similar qualitative behavior observed in viscoelastic fracture.The novelty of the present work lies in the use of Lip-field approach for the first time to model damage in viscoelastic materials. This can be considered as a first step to model damage softening in viscoelastic materials.

The future work will involve implementation of a viscoelastic damage model with unilateral effects within the Lip-field approach and to calibrate the model with experimental results. This will help to use the model for some real world applications.

# Références

[1] Lakes, R.S., Wineman, A., 2006. On Poisson's Ratio in Linearly Viscoelastic Solids. J Elasticity 85, 45–63. https ://doi.org/10.1007/s10659-006-9070-4

[2] D'Amico, F., Carbone, G., Foglia, M.M., Galietti, U., 2013. Moving cracks in viscoelastic materials : Temperature and energy-release-rate measurements. Engineering Fracture Mechanics 98, 315–325. https ://doi.org/10.1016/j.engfracmech.2012.10.026

[3] Pirmohammad, S., Ayatollahi, M.R., 2020. Fracture Behavior of Asphalt Materials, Structural Integrity. Springer International Publishing, Cham. https ://doi.org/10.1007/978-3-030-39974-0

[4] Knauss, W.G., 2015. A review of fracture in viscoelastic materials. Int J Fract 196, 99–146. https ://doi.org/10.1007/s10704-015-0058-6

[5] Schapery, R.A., 1984. Correspondence principles and a generalized J integral for large deformation and fracture analysis of viscoelastic media. Int J Fract 25, 195–223. https ://doi.org/10.1007/BF01140837

[6] Schapery, R.A., 1990. On some path independent integrals and their use in fracture of nonlinear viscoelastic media. International Journal of Fracture 42 : 189-207, 1990

[7] Brinson, H.F., Brinson, L.C., 2015. Polymer Engineering Science and Viscoelasticity. Springer US, Boston, MA. https ://doi.org/10.1007/978-1-4899-7485-3

[8] Dubois, F., Petit, C., 2005. Modelling of the crack growth initiation in viscoelastic media by the $G\theta v$-integral. Engineering Fracture Mechanics 72, 2821–2836. https ://doi.org/10.1016/j.engfracmech.2005.04.003

[9] Belytschko, T. and Black, T. (1999), Elastic crack growth in finite elements with minimal remeshing. Int. J. Numer. Meth. Engng., 45 : 601-620. https ://doi.org/10.1002/(SICI)1097-0207(19990620)45 :5<601 : :AID-NME598>3.0.CO ;2-S

[10] Moës, N., Dolbow, J. and Belytschko, T. (1999), A finite element method for crack growth without remeshing. Int. J. Numer. Meth. Engng., 46 : 131-150. https ://doi.org/10.1002/(SICI)1097-0207(19990910)46 :1<131 : :AID-NME726>3.0.CO ;2-J

[11] H.H. Zhang, L.X. Li. Modeling inclusion problems in viscoelastic materials with the extended finite element method. Finite Elements in Analysis and Design. Volume 45, Issue 10, 2009. Pages 721-729. https ://doi.org/10.1016/j.finel.2009.06.006.

[12] H.H. Zhang, G. Rong, L.X. Li. Numerical study on deformations in a cracked viscoelastic body with the extended finite element method. Engineering Analysis with Boundary Elements. Volume 34, Issue 6. 2010. Pages 619-624. https ://doi.org/10.1016/j.enganabound.2010.02.001.

[13] D. Dugdale. Yielding of steel sheets containing slits. J. of the Mech. and Phys. of Sol., 8 :100–104, 1960

[14] G. Barenblatt. The mathematical theory of equilibrium cracks in brittle fracture. Advances in Applied Mechanics, 7 :55–129, 1962.

[15] Introduction to Continuum Damage Mechanics. L.M. Kachanov, Martinus Nijhoff, Dordrecht (1986)

[16] Jean Lemaitre. How to use damage mechanics. Nuclear Engineering and Design. Volume 80, Issue 2. 1984, Pages 233-245, https ://doi.org/10.1016/0029-5493(84)90169-9.

[17] C. Yoon, D.H. Allen, Damage dependent constitutive behavior and energy release rate for a cohesive zone in a thermoviscoelastic solid, Int.J. Fract. 96 (1) (1999) 55–74

[18] P. Rahulkumar, A. Jagota, S.J. Bennison, S. Saigal, Cohesive element modeling of viscoelastic fracture : application to peel testing of polymers, Int. J. Solids Struct. 37 (13) (2000) 1873–1897

[19] E. Lorentz and S. Andrieux. Analysis of non-local models through energetic formulations. Int. J. of Sol. and Struc., 40 :2905–2936, 2003.

[20] G. Pijaudier-Cabot and Z. Bazant. Non-local damage theory. J. of Eng. Mech., 113 :1512–1533, 1987.

[21] C. Miehe, F. Welschinger, and M. Hofacker. Thermodynamically consistent phase-field models of fracture : Variational principles and multi-field FE implementations. Int. J. For Num. Meth. in Eng., 83(10) :1273–1311, 2010.

[22] M. Ambati, T. Gerasimov, and L. De Lorenzis. Phase-field modeling of ductile fracture. Comp. Mech., 55(5) :1017–1040, 2015.

[23] N. Moes, C. Stolz, P.-E. Bernard, and N. Chevaugeon. A level set based model for damage growth : The thick level set approach. Int. J. For Num. Meth. in Eng., 86 :358–380, 2011.

[24] Benjamin Shiferaw, Olivier Chupin, Jean-Michel Piau, Nicolas Moës. Development of a damage viscoelastic model using the thick level set approach to fracture : 1D modeling and comparison to uniaxial tension stress tests on bituminous specimens, Engineering Fracture Mechanics, Volume 257, 2021,108026. https ://doi.org/10.1016/j.engfracmech.2021.108026.

[25] Shen, R., Waisman, H., Guo, L., 2019. Fracture of viscoelastic solids modeled with a modified phase field method. Computer Methods in Applied Mechanics and Engineering 346, 862–890. https ://doi.org/10.1016/j.cma.2018.09.018

[26] Yin, B., Storm, J., Kaliske, M., 2021. Viscoelastic phase-field fracture using the framework of representative crack elements. Int J Fract. https ://doi.org/10.1007/s10704-021-00522-1

[27] Dammaß, F., Ambati, M., Kästner, M., 2021. A unified phase-field model of fracture in viscoelastic materials. Continuum Mech. Thermodyn. 33, 1907–1929. https ://doi.org/10.1007/s00161-021-01013-3

[28] Moes, N., Chevaugeon, N., 2021. Lipschitz regularization for softening material models : the Lip-field approach. Comptes Rendus. Mécanique 349, 415–434. https ://doi.org/10.5802/crmeca.91

[29] Chevaugeon, N., Moes, N., 2021. Lipschitz regularization for fracture : the Lip-field approach. arXiv :2111.04771 [cs].

[30] P. Germain, P. Suquet, and Q. S. Nguyen. Continuum thermodynamics. ASME Journal of Applied Mechanics, 50 :1010–1020, Dec. 1983.

[31] B. Halphen and Q.-S. Nguyen. Sur les materiaux standards généralisés. Journal de Mécanique , 14(1) :39–63, 1975.

[32] Williams, Malcolm L. ; Landel, Robert F. ; Ferry, John D. "The Temperature Dependence of Relaxation Mechanisms in Amorphous Polymers and Other Glass-forming Liquids". J. Amer. Chem. Soc. (1955)

[33] Lahellec, N., Suquet, P., 2007. On the effective behavior of nonlinear inelastic composites : I. Incremental variational principles. Journal of the Mechanics and Physics of Solids 55, 1932–1963. https ://doi.org/10.1016/j.jmps.2007.02.003

[34] Jirásek, M., 2002. Objective modeling of strain localization. Revue Française de Génie Civil 6, 1119–1132. https ://doi.org/10.1080/12795119.2002.9692735

[35] M. Andersen and L. Vandenberghe. The cvxopt linear and quadratic cone program solvers. https ://cvxopt.org/.